

Surface potential measurements by the dissipative force modulation method

Takeshi Fukuma

Department of Electronic Science and Engineering, Kyoto University, Kyoto 606-8501, Japan

Kei Kobayashi

International Innovation Center, Kyoto University, Kyoto 606-8501, Japan

Hirofumi Yamada^{a)} and Kazumi Matsushige

Department of Electronic Science and Engineering, Kyoto University, Kyoto 606-8501, Japan

(Received 21 June 2004; accepted 20 August 2004; published 29 October 2004)

In this study, we propose a novel surface property measurement technique using noncontact atomic force microscopy (NC-AFM), which is referred to as the “dissipative force modulation (DM) method.” NC-AFM-based surface property measurements have mostly utilized conservative tip-sample interaction forces, which induce a frequency shift of cantilever resonance without dissipating cantilever vibration energy. In the DM method, local surface properties are measured by detecting a modulated dissipative tip-sample interaction force which dissipates cantilever vibration energy and hence induces an amplitude variation in cantilever vibration. Since the force sensitivity to dissipative interactions obtained in a typical NC-AFM setup is much higher than that to conservative ones, the DM method can improve the sensitivities of conventional NC-AFM-based techniques that utilize conservative interactions. Combining this method with Kelvin-probe force microscopy, we present the first quantitative surface potential measurement through dissipative tip-sample interactions. © 2004 American Institute of Physics. [DOI: 10.1063/1.1805291]

I. INTRODUCTION

Noncontact atomic force microscopy (NC-AFM) using the frequency modulation (FM) detection method¹ has attracted much attention due to its capability of imaging atomic-scale structures even on insulating surfaces² as well as on conductive surfaces.^{3,4} In addition to the imaging of surface structures, NC-AFM has also been used for the investigation of local surface properties at a nanometer-scale resolution. In particular, Kelvin-probe force microscopy (KFM) combined with NC-AFM (Ref. 5) has been applied to the measurement of local surface potential distributions at a nearly atomic-scale resolution.

In NC-AFM, a microfabricated cantilever with a sharp tip mounted at its end is brought close to the surface to detect various tip-sample interaction forces. These tip-sample interaction forces detected in NC-AFM are classified into two categories: “conservative” forces and “dissipative” forces.^{6,7} Conservative forces induce a frequency shift of cantilever resonance without dissipating cantilever vibration energy. On the other hand, dissipative forces reduce cantilever vibration amplitude, which means that the mechanical energy of the cantilever is dissipated through some of the tip-sample interactions.

Since tip-sample interaction forces in NC-AFM are mostly conservative, conservative forces, rather than dissipative forces, have been utilized thus far in NC-AFM applications. The frequency shift induced by a conservative tip-

sample interaction force is detected and used for tip-sample distance regulation. In KFM, an ac bias voltage is applied between a tip and a sample, which modulates the magnitude of a conservative electrostatic force. Then the resultant change in cantilever resonance frequency is detected and used for bias feedback regulation.⁵

In contrast to the conservative force measurements, surface property measurements hardly use dissipative forces. This is because energy dissipation in NC-AFM has different origins related to the electrical and mechanical properties of a tip and a sample.^{8,9} Thus, the quantitative evaluation of surface properties is difficult by a simple measurement of the total amount of energy dissipation. However, previously reported energy dissipation values measured by NC-AFM have suggested that the force sensitivity to dissipative interactions obtained with a typical NC-AFM setup is much higher than that to conservative ones.^{10,11} For example, an energy dissipation of less than 1 fW was accurately measured in previous studies,^{10,11} which means that a dissipative electrostatic force of less than 0.01 pN is readily detected in NC-AFM. This indicates that the use of dissipative forces instead of conservative ones should improve such sensitivity in surface property measurements.

In this article, we propose a novel NC-AFM-based technique referred to as the “dissipative force modulation (DM) method.” By introducing and detecting a modulated dissipative force, the method enables the separation of the dissipative interaction of interest. Combining this method with KFM, we have developed a modified type of KFM that enables quantitative surface potential measurement with an ex-

^{a)}Electronic mail: h-yamada@kuee.kyoto-u.ac.jp

tremely high sensitivity. To show the clear contrast between the currently used KFM and the newly developed one, we hereafter describe these two methods as conservative force modulation KFM (CM-KFM) and dissipative force modulation KFM (DM-KFM), respectively. In this article, the basic principle and experimental setup of DM-KFM are presented. The extremely high sensitivity of NC-AFM to a dissipative interaction force is experimentally demonstrated. In addition, the preliminary results of surface potential measurements using DM-KFM are presented.

II. BASIC PRINCIPLE

A. Conservative and dissipative forces

In NC-AFM, the phase difference between cantilever oscillation and its excitation signal (v_{exc}) is continuously kept constant at 90° with a self-excitation circuit. Thus, v_{exc} and tip position (z_t) can be described as

$$v_{\text{exc}} = V_{\text{exc}} \cos(\omega t), \quad (1)$$

$$z_t = z_{t0} + A \sin(\omega t). \quad (2)$$

V_{exc} and ω are the amplitude and frequency of the cantilever excitation signal, respectively. z_{t0} and A denote the mean tip position and the amplitude of the cantilever vibration, respectively.

Due to the high Q -factor of the cantilever, cantilever motion, particularly in vacuum, is predominantly affected by the ω -components of tip-sample interaction forces. Accordingly, the tip-sample interaction force (F_{ts}) can be approximately described by two trigonometric functions whose phases differ by 90° ,

$$F_{ts} = F_{ts,c} \sin(\omega t) + F_{ts,d} \cos(\omega t). \quad (3)$$

The first component ($F_{ts,c} \sin(\omega t)$) changes with the same phase as that of the cantilever vibration, which induces a frequency shift (Δf) of cantilever resonance without dissipating vibration energy. On the other hand, the second component ($F_{ts,d} \cos(\omega t)$) changes with the same phase as that of the cantilever excitation signal, which dissipates some energy of the cantilever vibration. The energy dissipation results in an amplitude variation (ΔA) of the cantilever oscillation. In this article, we refer to the former component as conservative force and to the latter as dissipative force.

From the equation of motion, Δf and ΔA are given by

$$\Delta f = -\frac{f_0}{2kA} F_{ts,c}, \quad (4)$$

$$\Delta A = \frac{Q}{k} F_{ts,d}, \quad (5)$$

where f_0 , k , and Q are the resonance frequency, the spring constant and the Q -factor of the cantilever, respectively. Thus, the minimum detectable force for conservative interactions ($\delta F_{ts,c}$) and that for dissipative interactions ($\delta F_{ts,d}$) are given by

$$\delta F_{ts,c} = \frac{2kA}{f_0} \delta f, \quad (6)$$

TABLE I. Typical values of parameters of cantilever under vacuum and experimental conditions in NC-AFM experiments.

Parameter	Value	Unit
f_0	300	kHz
k	40	N/m
Q	30 000	
T	300	K
f_m	1	kHz
B	200	Hz
n_{ds}	0.1–1	pm/ $\sqrt{\text{Hz}}$
A	5	nm
z_{t0}	6	nm
R	5	nm

$$\delta F_{ts,d} = \frac{k}{Q} \delta A, \quad (7)$$

where δf and δA are the minimum detectable frequency and amplitude, respectively.

There are two major noise sources that limit the sensitivities to frequency and amplitude in NC-AFM, which are the thermal vibration of the cantilever and noise from the deflection sensor. In both CM- and DM-KFM, a conservative force or a dissipative electrostatic force is modulated at a frequency of f_m by applying an ac bias voltage ($f_m \ll f_0$). Thus, the spectral noise density of a cantilever deflection signal at a frequency of $f_0 + f_m$ has to be taken into account for the evaluation of the force sensitivities. For the noise arising from the cantilever thermal vibration, the root-mean-square (RMS) value of spectral noise density (n_{th}) at a frequency of $f_0 + f_m$ is approximately expressed by¹

$$n_{\text{th}} = \sqrt{\frac{k_B T f_0}{2\pi k Q f_m^2}}. \quad (8)$$

Table I shows an example of typical cantilever parameters under vacuum and experimental conditions. Under these conditions, n_{th} is 13 fm/ $\sqrt{\text{Hz}}$. On the other hand, the typical RMS value of the spectral noise density arising from a deflection sensor (n_{ds}) falls in the range of 0.1–1 pm/ $\sqrt{\text{Hz}}$, which is much larger than n_{th} . Thus, n_{ds} predominantly determines δf and δA for typical NC-AFM setups operating in vacuum.

Assuming that the modulated frequency and amplitude are detected with a lock-in amplifier with a bandwidth of B , δf , and δA at a modulation frequency of f_m are, respectively, given by¹²

$$\delta f = \frac{\sqrt{12}}{\pi A} f_m n_{\text{ds}} \sqrt{B}, \quad (9)$$

$$\delta A = n_{\text{ds}} \sqrt{B}. \quad (10)$$

Note that the condition $f_m^2 \gg B^2$ is assumed in obtaining δf . With the typical conditions given in Table I, δf is approximately 0.3–3 Hz while δA is approximately 1.4–14 pm.

From Eqs. (6), (7), (9), and (10), $\delta F_{ts,c}$ and $\delta F_{ts,d}$ are, respectively, obtained as

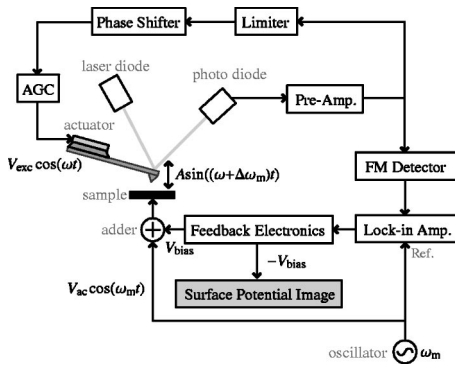


FIG. 1. Schematic of experimental setup for CM-KFM. The frequency variation induced by the modulated conservative electrostatic force is detected for obtaining V_{CPD} .

$$\delta F_{tsC} = \frac{4\sqrt{3}k f_m}{\pi f_0} n_{ds} \sqrt{B}, \quad (11)$$

$$\delta F_{tsd} = \frac{k}{Q} n_{ds} \sqrt{B}. \quad (12)$$

Under the typical conditions shown in Table I, δF_{tsC} is approximately 0.4–4 pN while δF_{tsd} is approximately 2–20 fN. Therefore, owing to the high Q -factor of the cantilever in vacuum, the force sensitivity to dissipative interactions obtained with a typical NC-AFM setup is much higher than that to conservative ones.

B. Conservative force modulation method

When a dc bias voltage is applied between a tip and a sample, the induced electrostatic force (F_{es}) changes with the same frequency and phase as those of the cantilever vibration. This is because F_{es} is a function of tip position which changes according to Eq. (2). Thus, the induced electrostatic force is naturally conservative. In CM-KFM, a bias voltage oscillating with a frequency (ω_m) much lower than that of the cantilever vibration is applied between the tip and the sample for introducing a modulated conservative electrostatic force.

Figure 1 shows an experimental setup for CM-KFM. In CM-KFM, an ac bias voltage $V_{ac} \cos(\omega_m t)$ and a dc bias voltage V_{bias} is applied between a tip and a sample. Accordingly, the tip-sample potential difference V_{ts} is given by

$$V_{ts} = V_{dc} + V_{ac} \cos(\omega_m t), \quad (13)$$

where

$$V_{dc} = V_{bias} + V_{CPD}. \quad (14)$$

Here V_{CPD} is the contact potential difference between the tip and the sample and V_{dc} is defined as the sum of V_{bias} and V_{CPD} .

F_{es} induced by V_{ts} is given by¹³

$$F_{es} = -\frac{\pi \epsilon_0 R}{z_t} V_{ts}^2, \quad (15)$$

where ϵ_0 and R are the dielectric constant in vacuum and the tip radius, respectively. Using Eq. (2), the equation is rewritten as

$$F_{es} = -\frac{\pi \epsilon_0 R}{z_{t0}} \left[1 - \frac{A}{z_{t0}} \sin(\omega t) \right] V_{ts}^2, \quad (16)$$

where we assume that $A \ll z_{t0}$. Although this assumption is not always satisfied in conventional NC-AFM, we have checked that no significant difference was made in the following discussion even without this assumption. Thus, we still keep it to have the essential understanding by simple calculation. From Eq. (16), the conservative electrostatic force (F_{esc}) is given by

$$F_{esc} = \frac{\pi \epsilon_0 R A}{z_{t0}^2} V_{ts}^2, \quad (17)$$

while the dissipative electrostatic force (F_{esd}) is zero.

From Eqs. (4), (13), and (17), the ω_m component of the frequency shift (Δf_m) induced by the electrostatic interaction is given by

$$\Delta f_m = -\frac{\pi \epsilon_0 R f_0 V_{ac}}{k z_{t0}^2} V_{dc} \cos(\omega_m t). \quad (18)$$

This frequency variation is detected with a lock-in amplifier from the output signal of a frequency modulation (FM) detector. Then the detected signal is fed into the feedback electronics that controls V_{bias} so as to make V_{dc} zero. Consequently, the surface potential image is obtained by recording $-V_{bias}$ as the tip is scanning over a surface.

From Eqs. (9) and (18), the minimum detectable contact potential difference δV_{CPD} is given by

$$\delta V_{CPD} = \frac{2\sqrt{6}}{\pi^2 \epsilon_0 R A V_{ac}} \frac{k z_{t0}^2 f_m}{f_0} n_{ds} \sqrt{B}. \quad (19)$$

Using the typical conditions given in Table I, δV_{CPD} is approximately 15–150 mV at V_{ac} of 1 V. In other words, to obtain a potential resolution higher than 10 mV, V_{ac} has to be higher than 1 V.

The application of an ac bias voltage also produces a dc component of the frequency shift (Δf_{dc}) as well as the ω_m component. This dc component remains even when the bias feedback regulation reaches a steady state ($V_{dc}=0$) and is given by

$$\Delta f_{dc} = -\frac{\pi \epsilon_0 R f_0}{4k z_{t0}^2} V_{ac}^2. \quad (20)$$

Under the typical conditions shown in Table I, Δf_{dc} is 7.2 Hz at $V_{ac}=1$ V. This value is not negligible compared with the typical frequency shift values used for topographic imaging, which ranges from 10 to 100 Hz. Thus, Δf_{dc} can cause topographic artifacts as previously reported.¹⁴ In particular, for KFM applications to insulating thin films, such as organic thin films, on metal surfaces, z_{t0} should be defined as the distance between the metal surface and the tip position. In addition, the dielectric constant between the tip and the metal surface can vary depending on the type of film material. Accordingly, site-dependent variations in z_{t0} and dielectric constant can result in topographic artifacts due to the variation in Δf_{dc} . This is one of the major problems in CM-KFM.

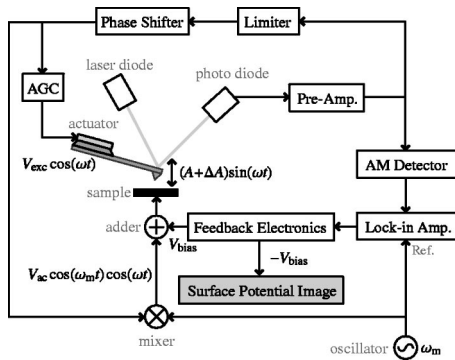


FIG. 2. Schematic of experimental setup for DM-KFM, which can be obtained with only small modifications of that for CM-KFM. The amplitude variation induced by the modulated dissipative electrostatic force is detected for obtaining V_{CPD} .

C. Dissipative force modulation method

Since the electrostatic force in a simple CM-KFM setup is conservative, we need to modify the setup to detect F_{es} as the dissipative force (F_{esd}). The required dissipative force must have the same frequency as that of the cantilever oscillation but a 90° phase difference. The cantilever excitation signal in a self-excitation circuit which coincides with these conditions can be an appropriate candidate for generating the dissipative force. In DM-KFM, F_{esd} is introduced by applying an ac bias voltage synchronized with the cantilever excitation signal. Then the amplitude of the ac bias voltage is modulated at a frequency (ω_m) much lower than that of the cantilever vibration (ω), producing a modulated dissipative electrostatic force.

Figure 2 shows an experimental setup for DM-KFM. Note that the tip-sample distance is regulated in the constant frequency shift mode although this part of the setup is omitted in Fig. 2 to avoid complication. In DM-KFM, an ac bias voltage $V_{ac} \cos(\omega_m t) \cos(\omega t)$ and a dc bias voltage V_{bias} are applied between the tip and the sample. The resultant tip-sample potential difference V_{ts} is given by

$$V_{ts} = V_{dc} + V_{ac} \cos(\omega_m t) \cos(\omega t). \quad (21)$$

Note that V_{dc} has been defined in Eq. (14). From Eqs. (14), (16), and (21), the electrostatic force (F_{es}) produced by the application of the bias voltage is given by

$$F_{es} = \frac{\pi \epsilon_0 R A}{z_{t0}^2} \left[V_{dc}^2 + \frac{1}{8} V_{ac}^2 \{1 + \cos(2\omega_m t)\} \right] \sin(\omega t) - \frac{2\pi \epsilon_0 R}{z_{t0}} V_{ac} V_{dc} \cos(\omega_m t) \cos(\omega t), \quad (22)$$

where we take the components with the first order of $\sin(\omega t)$ or $\cos(\omega t)$ into account.

The second term on the right-hand side of Eq. (22) corresponds to the dissipative electrostatic force which induces amplitude variation (ΔA) described by

$$\Delta A = -\frac{2\pi \epsilon_0 R Q}{z_{t0} k} V_{ac} V_{dc} \cos(\omega_m t). \quad (23)$$

The amplitude variation is detected with a lock-in amplifier from the output signal of an amplitude modulation (AM) detector with a bandwidth larger than ω_m . The detected sig-

nal is fed into the feedback electronics that control V_{bias} for canceling out the ω_m component of amplitude variation. Consequently, V_{bias} is kept equal to $-V_{CPD}$. Thus, a surface potential image can be obtained by two-dimensionally mapping the values of $-V_{bias}$.

From Eqs. (10) and (23), the minimum detectable contact potential difference (δV_{CPD}) is given by

$$\delta V_{CPD} = \frac{1}{\sqrt{2} \pi \epsilon_0 R Q V_{ac}} k z_{t0} n_{ds} \sqrt{B}. \quad (24)$$

Under the typical conditions shown in Table I, δV_{CPD} is 0.58–5.8 mV at a V_{ac} of 0.1 V. That is, V_{ac} of 0.1 V is sufficiently high for obtaining a potential resolution of 10 mV. Owing to the high force sensitivity of DM-KFM, we can achieve a sufficient potential resolution with smaller V_{ac} values than those required for CM-KFM.

The first term on the right-hand side of Eq. (22) represents the conservative electrostatic force that causes a frequency shift of the cantilever resonance. The dc frequency shift (Δf_{dc}) in a steady state under the bias feedback control ($V_{bias} = -V_{CPD}$) is given by

$$\Delta f_{dc} = -\frac{\pi \epsilon_0 R f_0}{16 k z_{t0}^2} V_{ac}^2. \quad (25)$$

Comparing this equation with Eq. (20), one can find that Δf_{dc} in DM-KFM is 1/4 that in CM-KFM. In addition, Δf_{dc} can be decreased to a negligible value because small V_{ac} values are available in DM-KFM. For example, under the typical conditions shown in Table I, Δf_{dc} is 0.018 Hz at V_{ac} of 0.1 V. The result shows that DM-KFM enables high resolution potential measurements without inducing topographic artifacts. The reduction in V_{ac} is also beneficial for suppressing the influence of bias voltage on sample properties to be measured by KFM.

III. RESULTS AND DISCUSSIONS

A. Signal-to-noise ratio measurements

Although the previously reported energy dissipation values obtained with NC-AFM have suggested that the force sensitivity of NC-AFM to dissipative interactions is higher than that to conservative ones,^{10,11} quantitative comparison between these two force sensitivities has not yet been performed. In this study, we even compared the signal-to-noise ratio (SNR) of FM- and AM-detected signals generated by conservative and dissipative electrostatic forces at different bias modulation frequencies.

For the conservative force measurement, an ac bias voltage of $V_{ac} \cos(\omega_m t)$ was applied between the tip and the sample and the modulated frequency shift was detected with an FM detector. On the other hand, for the dissipative force measurement, an ac bias voltage of $V_{ac} \cos(\omega_m t) \cos(\omega t)$ was applied and the induced amplitude variation was detected with an AM detector. The bandwidths of the FM and AM detectors were 1 kHz. A commercially available ultrahigh vacuum (UHV) NC-AFM (JEOL: JSPM-4500) was used. A homebuilt PLL circuit using a voltage-controlled crystal oscillator (VCXO) (Ref. 15) was used for FM detection while an RMS-DC converter was used for AM detection. SNR was

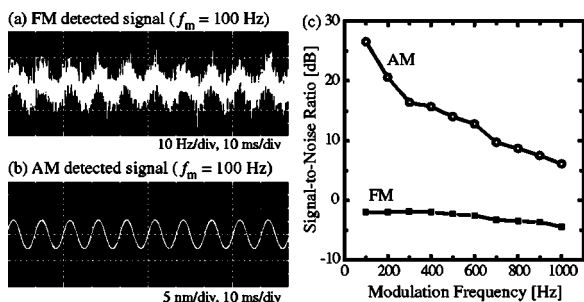


FIG. 3. (a), (b) Waveforms of FM- and AM-detected signals at modulation frequency of 100 Hz. (c) SNRs of FM- and AM-detected signals plotted as functions of modulation frequency ($V_{ac}=0.1$ V, $V_{bias}=1.0$ V, $A=5$ nm, $\Delta f=-20$ Hz).

measured with an FFT analyzer (softDSP: SDS-200). The cantilever was a Pt-coated Si cantilever (Nanosensors: NCHPt) with a nominal spring constant of 40 N/m and a resonance frequency of approximately 300 kHz. The Q -factor measured under UHV conditions was approximately 30 000. The sample was a Pt thin film deposited on a SiO_2/Si substrate. The measurements were performed at a tip position where $\Delta f=-20$ Hz. V_{bias} and V_{ac} were set at 1.0 V and 0.1 V, respectively.

Figures 3(a) and 3(b) show the waveforms of FM- and AM-detected signals obtained at a modulation frequency of 100 Hz, respectively. These waveforms reveal that the AM-detected signal has a much higher SNR than the FM-detected signal. This result experimentally demonstrates that the force sensitivity of NC-AFM to dissipative interactions is much higher than that to conservative ones. Figure 3(c) shows the frequency dependences of the SNRs of AM- and FM-detected signals. The result indicates that the SNR of the AM-detected signal decreases with increasing modulation frequency while the SNR of the FM-detected signal remains almost constant. However, the result also shows that the AM-detected signal still exhibits a higher SNR than the FM-detected signal even at a modulation frequency of 1 kHz.

The amplitude variation induced by a dissipative force settles on a time scale of $\tau_{AM} \approx 2Q/f_0$ while the response time for the frequency variation induced by a conservative force is given by $\tau_{FM} \approx 1/f_0$.¹² Namely, AM detection has a slower time response by a factor of Q than that of FM detection, which decreases force sensitivity to dissipative forces at higher modulation frequencies. Thus, the DM method is most effective for applications that require an extremely high force sensitivity but not a very high scanning speed. The use of a high-resonance-frequency cantilever is the most effective way of enhancing force sensitivity and improving the time response of AM detection.

B. Surface potential imaging

Using DM- and CM-KFM, we have measured the surface potential distribution of a dimethylquinquethiophene (M5T) monolayer formed on a Pt surface. M5T molecules [Fig. 4(a)] deposited on a Pt surface form monolayer islands with their molecular axes perpendicular to the surface, as shown in Fig. 4(b). It has been reported that these monolayer

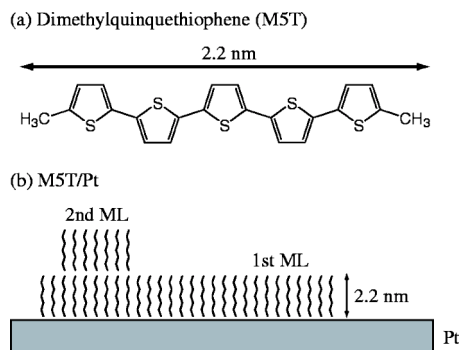


FIG. 4. (Color online) (a) Molecular structure of the M5T molecule. (b) Schematic model of the M5T monolayer formed on a Pt surface.

islands have 100–200 mV higher surface potential than Pt surfaces.¹⁶

Figure 5 shows the topographic and potential images taken by CM- and DM-KFM. The film/substrate potential difference measured from these two potential images [(Figs. 5(b) and 5(d))] agreed well and the value was approximately 100 mV. Owing to the excellent SNR of AM detection, the potential image obtained by DM-KFM shows a much clearer contrast than the CM-KFM image. Namely, the result demonstrates that DM-KFM has a higher potential resolution than CM-KFM.

In CM-KFM, it was difficult to obtain a clear surface potential image with V_{ac} values of less than approximately 1 V while clear potential contrast was obtained in DM-KFM even with V_{ac} of 0.1 V as shown in Fig. 5(d). The result shows that DM-KFM enables us to achieve a sufficiently high potential sensitivity even with a small V_{ac} , markedly suppressing the possible formation of topographic artifacts and the influence of the bias application on the sample properties. DM-KFM is also suitable for NC-AFM operation with a small cantilever vibration amplitude, which has been recently proven to be beneficial for enhancing spatial resolution in topographic imaging.¹⁷ δV_{CPD} for CM-KFM increases

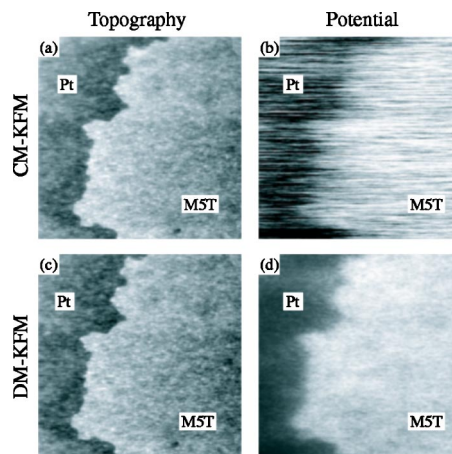


FIG. 5. (Color online) NC-AFM images of the M5T monolayer on a Pt surface. (a) Topographic and (b) potential images obtained by CM-KFM. (c) Topographic and (d) potential images obtained by DM-KFM. The experimental parameters used in both CM- and DM-KFM: $\Delta f=-20$ Hz, $A=1$ nm, $V_{ac}=0.1$ V, $f_m=1$ kHz. The scanned area and imaging speed were $1 \mu\text{m} \times 1 \mu\text{m}$ and 15 min/frame, respectively.

with decreasing cantilever vibration amplitude while that of DM-KFM remains almost constant as expected from Eqs. (19) and (24).

In terms of the spatial resolution of a potential image, CM-KFM has an advantage over DM-KFM. Comparing Eqs. (18) and (23), we can find that Δf_m is proportional to $1/z_{r0}^2$ while ΔA changes in proportion to $1/z_{r0}$. Thus, DM-KFM is more sensitive to long-range interaction force than CM-KFM. If we use an ac bias voltage of $V_{ac} \cos(\omega_m t) \cot(\omega t)$ instead of $V_{ac} \cos(\omega_m t) \cos(\omega t)$, we would be able to make ΔA proportional to $1/z_{r0}^2$. In that case, however, a high-voltage pulse will be intermittently applied between a tip and a sample, which may influence the sample properties to be measured by KFM.

In this study, we applied the DM method to surface potential measurements by KFM. However, the DM method can be applied to not only KFM but also other surface property measurements such as magnetic force microscopy and photo induced force microscopy.¹⁸

ACKNOWLEDGMENTS

This work was supported by a Grant-in-Aid from the Ministry of Education, Culture, Sports, Science and Technology of Japan and the 21st Century Center of Excellence Program, Kyoto University. The authors would like to thank S. Hotta (Kyoto Institute of Technology) for providing M5T molecules.

- ¹T. R. Albrecht, D. H. P. Grütter, and D. Ruger, *J. Appl. Phys.* **69**, 668 (1991).
- ²M. Bammerlin, R. Lüthi, E. Meyer, A. Baratoff, J. Lü, M. Guggisberg, C. Gerber, L. Howald, and H.-J. Güntherodt, *Probe Microsc.* **1**, 3 (1997).
- ³F. J. Giessibl, *Science* **267**, 68 (1995).
- ⁴S. Kitamura and M. Iwatsuki, *Jpn. J. Appl. Phys., Part 2* **34**, L1086 (1995).
- ⁵S. Kitamura and M. Iwatsuki, *Appl. Phys. Lett.* **72**, 3154 (1998).
- ⁶B. Gotsmann, C. Seidel, B. Anczykowski, and H. Fuchs, *Phys. Rev. B* **60**, 11051 (1999).
- ⁷M. Guggisberg, M. Bammerlin, C. Loppacher, O. Pfeiffer, A. A. adn, V. Barwich, R. Bennewitz, A. Baratoff, E. Meyer, and H.-J. Güntherodt, *Phys. Rev. B* **61**, 11151 (2000).
- ⁸W. Denk and D. W. Pohl, *Appl. Phys. Lett.* **59**, 2171 (1991).
- ⁹R. Bennewitz, A. S. Foster, L. N. Kantrovich, M. Bammerlin, C. Loppacher, S. Schär, M. Guggisberg, and E. Meyer, *Phys. Rev. B* **62**, 2074 (2000).
- ¹⁰C. Loppacher, R. Bennewitz, O. Pfeiffer, M. Guggisberg, M. Bammerlin, S. Schär, V. Barwich, A. Baratoff, and E. Meyer, *Phys. Rev. B* **62**, 13674 (2000).
- ¹¹T. Fukuma, K. Umeda, K. Kobayashi, H. Yamada, and K. Matsushige, *Jpn. J. Appl. Phys., Part 1* **41**, 4903 (2002).
- ¹²F. J. Giessibl, *Noncontact Atomic Force Microscopy (Nanoscience and Technology)* (Springer, Berlin, 2002), Chap. 2.
- ¹³L. Olsson, N. Lin, V. Yakimov, and R. Erlandsson, *J. Appl. Phys.* **84**, 4060 (1998).
- ¹⁴K. Okamoto, Y. Sugawara, and S. Morita, *Appl. Surf. Sci.* **188**, 381 (2002).
- ¹⁵K. Kobayashi, H. Yamada, H. Itoh, T. Horiuchi, and K. Matsushige, *Rev. Sci. Instrum.* **72**, 4383 (2001).
- ¹⁶K. Umeda, K. Kobayashi, K. Ishida, S. Hotta, H. Yamada, and K. Matsushige, *Jpn. J. Appl. Phys., Part 1* **40**, 4381 (2001).
- ¹⁷F. J. Giessibl, H. Bielefeldt, S. Hembacher, and J. Mannhart, *Appl. Surf. Sci.* **140**, 352 (1999).
- ¹⁸M. Abe, T. Uchihashi, M. Ohta, H. Ueyama, Y. Sugawara, and S. Morita, *J. Vac. Sci. Technol. B* **15**, 1512 (1997).